Macromolecules

pubs.acs.org/Macromolecules Article

Synthesis, Characterization, and Application of High-Molecular-Weight Polyethylene-like Polycarbonates: Toward Sustainable and Recyclable Fibers

Mingfu Zheng, Wenjun Peng, Yao-Yao Zhang,* Xianming Zhang,* and Wenxing Chen

Cite This: Macromolecules 2024, 57, 7020−7030 Read Online

ACCESS | Metrics & More | Article Recommendations | Supporting Information

ABSTRACT: Polyethylene-like materials, such as polyethylene-like polycarbonates (PLPCs), have garnered widespread attention because they can compensate for the nondegradability of polyethylene while maintaining mechanical properties resembling polyethylene. Although substantial efforts have been invested to develop synthetic methods of PLPCs, a long-pursued goal is to apply these polymers that either functionally replace or exhibit performance advantages relative to incumbent polymers. Herein, we presented a scalable synthesis of PLPCs from long-chain α,ω-diols and diphenyl carbonate, studied the relationship between the structure and properties, and expanded their practical applications as high-strength and high-toughness fibers. These PLPCs were prepared using equivalent biobased aliphatic diols and diphenyl carbonate via melt polycondensation using NaOH/PPh_4OPh as catalysts at ppm levels, showing high molecular weight (92,000−121,000 g/mol) and narrow distribution (1.69−1.80) with high yield (~99%). The influence of the carbonate unit density on thermodynamic properties, morphology, and mechanical performance was systematically studied. The fibers prepared from longer-methylene-sequence PLPCs (PC10, PC12, and PC14) show reliable mechanical properties such as satisfactory tensile modulus and yield stress as well as toughness, while the fibers of shorter-methylene-sequence PC6 and PC8 present compromised mechanism properties due to the higher carbonate densities influencing the packed crystalline structure. These affordable and easy-to-prepare PLPC materials also show excellent chemical and physical recovery capabilities, holding great potential for further practical applications.

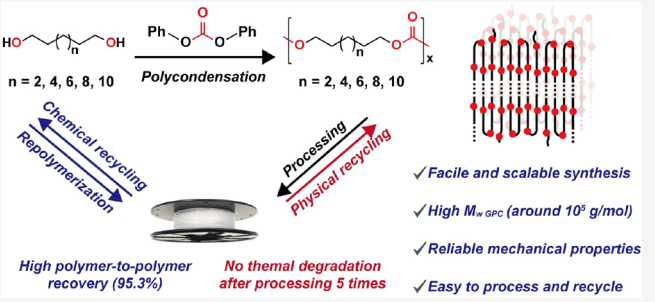

INTRODUCTION

Plastics are a mainstay in various technological fields of human society with about 400 million metric tons produced annually, surpassing most other man-made materials.[1] Polyethylene (PE), as the most abundantly produced plastic, accounting for about one-third of the overall annual production of plastics,[2,3] plays a vital role in modern society as fibers, films, and engineering plastics.[4−6] The tightly packed long chains of PE lead to a high degree of crystallinity, contributing to its outstanding material properties such as chemical stability and corrosion resistance. Nevertheless, these properties make them difficult to degrade and recycle.[6,7] Additionally, the petrochemical origin of PE also raises world concern for fossil fuels (oil, natural gas, and coal).[8,9] As a result, polymeric materials that are recyclable and degradable and have mechanical properties similar to PE are drawing increasing attention.[10−13]

Introducing low densities of cleavage groups into PE chains to make PE-like polymers can endow them with degradability and recyclability while maintaining thermal and mechanical properties.[14,15] Ester, acetal, and carbonate functionalities have been successfully incorporated into the PE backbone via ring-opening polymerization of macrocyclic lactones,[16−18] acyclic diene metathesis of dienes or ring-opening metathesis polymerization of cyclic olefins,[19,20] and polycondensation of classical A_2 and B_2 monomers (Figure 1a).[21,22] Among these polymerization techniques, polycondensation presents an elegant strategy due to its abundant commercially available and affordable monomers, which grants easy access to tuning polymeric structures and the corresponding properties.[22,23] By employing long-chain α,ω-diols derived from vegetable oil derivatives,[24−27] Mecking and co-workers prepared corresponding long-chain PE-like polyesters, polyacetals, and polycarbonates with M_n over 10^4 g/mol.[19] The long-chain polycarbonates and polyester possess PE-like solid-state structures and, therefore, present good mechanical properties, holding great potential for further applications. Despite the fact that significant effort has been devoted to the synthesis and

Received: April 23, 2024
Revised: June 26, 2024
Accepted: July 22, 2024
Published: July 26, 2024

https://doi.org/10.1021/acs.macromol.4c00933
Macromolecules 2024, 57, 7020−7030

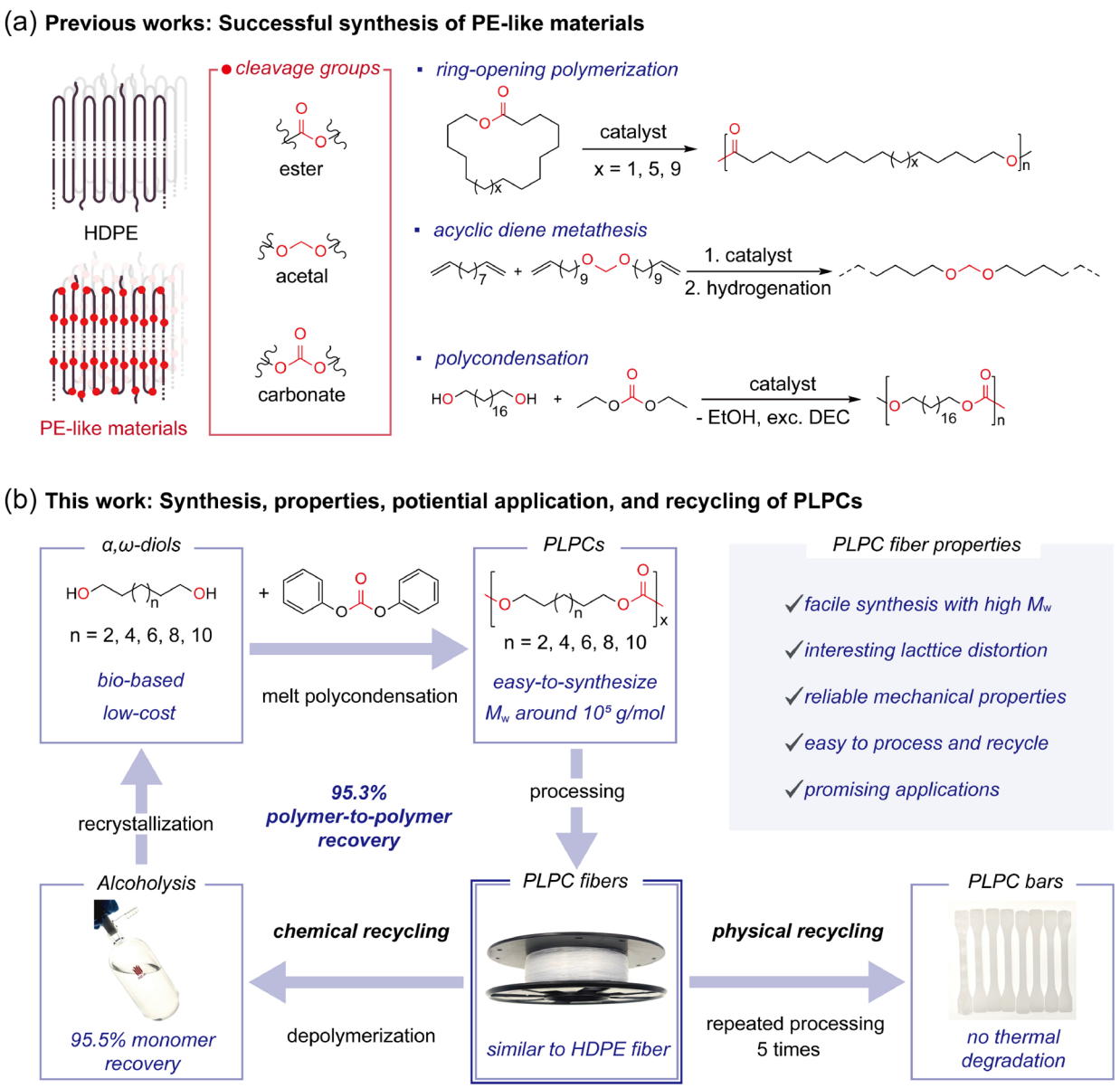

Figure 1. (a) Different PE-like materials synthesized by ring-opening polymerization, acyclic diene metathesis, and polycondensation methods. (b) This work: the systematic studies of PLPCs from synthesis, property characterization, fiber preparation, and their performance evaluation to their recycling.

degradation of PE-like materials,[28−30] a long-pursued target is to produce sustainable, inexpensive, and biobased PE-like materials to meet practical applications in a wide variety of fields. A prerequisite to realize this target is to establish a scalable, reliable, and economical synthesis strategy for PE-like materials, which is preferred if it is compatible with the current industrial synthesis process.

Among various PE-like polymers, PE-like polycarbonates (PLPCs) with in-chain carbonate units arouse our interest due to their excellent gas barrier property, strong resistance to acid, and neutral degradation products.[31−33] Currently, the preparation of PLPCs mainly relies on the polycondensation of *α,ω*-diols with much excess dialkyl carbonate using moisture-sensitive metal hydrides such as LiH (0.5−1.0 mol % loading) as a promoter. Due to the fact that the boiling point of dialkyl carbonate is lower than the transesterification reaction temperature, a large excess of dialkyl carbonate (2.5−5 equiv) is required. Furthermore, the molecular weight of the resultant PLPC can hardly exceed 10^5 g/mol.[34] Using diphenyl carbonate (DPC) as the carbonyl source could avoid the above problems, since DPC has a high boiling point and the byproduct phenol can be easily removed, which also helps to precisely control the desired molar ratio of end-groups. In fact, DPC is commonly used for the industrial production of bisphenol A polycarbonate.[35] Successful synthesis of several high-molecular-weight aliphatic polycarbonates (with ≤6 methylenes between two carbonate groups) has been achieved by using DPC as feedstocks, producing resultant polymers with molecular weight up to 10^5 g/mol.[36] Although the synthesis of PLPCs from DPC has not been reported in the literature, these previous works give confidence in using DPC as a carbonyl source to prepare high-quality PLPCs.

In addition to issues related to PLPC production, there is lacking a comprehensive understanding of the structure−performance relationships of PLPCs,[37,38] such as how the chain lengths of structural units influence the thermal and

https://doi.org/10.1021/acs.macromol.4c00933
Macromolecules 2024, 57, 7020−7030

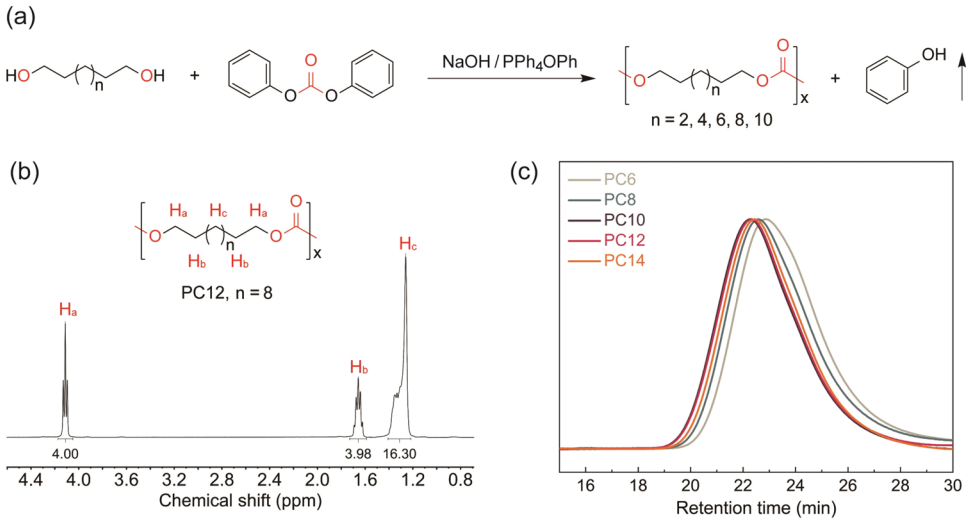

Figure 2. Synthesis and characterization of PLPCs. (a) Polycondensation of α,ω-diols and DPC to prepare PC6−PC14. (b) ^{1}H NMR spectrum of PC12. (c) GPC traces of the PLPCs.

mechanical properties and what is the critical methylene sequence length to maintain the PE-like properties. The obtained deep understanding is anticipated to guide the tuning of the structure and properties of PLPCs to meet the requirements for diverse applications. Notably, in the aspect of thermal and crystalline properties, Müller and Liu have made important contributions, revealing an interesting even−odd effect through systematic characterization of the crystallization behavior and structure, as well as the molecular conformation of aliphatic polycarbonates with different chain lengths (6−12 methylene groups).[39] Similarly, research to expand applications of PE-like polymers is also scant. A rare example is that Mecking's group applied the polyester-based and polycarbonate-based PE-like materials for common injection molding as PE, manifesting excellent promise of PE-like materials as substitutes for PE.[34] Given that PLPCs possess PE-like structure and high crystallinity, PLPCs are expected to be good materials for the preparation of polymer fibers that are widely used in textile and weaving applications and hold promise to be an alternative to existing non-degradable polymer fibers, making an important contribution to realizing a sustainable plastics economy.

In this work, systematic studies of PLPCs from synthesis, property characterization, fiber preparation, and performance evaluation, to their recycling, were performed. PLPCs with high molecular weight (up to 10^5 g/mol) and narrow distributions (1.69−1.80) were prepared by melt polycondensation of α,ω-diols (C6, C8, C10, C12, and C14) with DPC in high yields. The impact of the carbonate unit distribution in the molecular chain on the thermal performance, morphology characteristics, and melt flowability was then systematically studied. Furthermore, fibers of these PLPCs were first prepared by means of melt spinning and hot-drawing processes under optimized conditions. The long-methylene-sequence PLPC (PC10, PC12, and PC14) fibers exhibit satisfying tensile modulus, yield stress, and toughness, while the short-methylene-sequence PLPC (PC6 and PC8) fibers show compromised mechanical properties accompanied by interesting lattice distortion. These PLPCs also show excellent physical and chemical recyclability. These merits of PLPCs are expected to provide excellent and tunable performance in replacing current petrochemical plastics and fibers.

RESULTS AND DISCUSSION

PLPC Synthesis. High-molecular-weight (up to10^5 g/mol) PLPCs (PC6, PC8, PC10, PC12, and PC14) were prepared from long-chain α,ω-diols and DPC using NaOH/PPh_4OPh as catalysts with yields up to 99%. These α,ω-diols include1,6-hexanediol (C6), 1,8-octanediol (C8), 1,10-decanediol (C10), 1,12-dodecanediol (C12), and 1,14-tetradecanediol (C14). They can be obtained at low prices to meet the cost requirements for application promotion, and they can be biosynthesized from renewable free fatty acids.[40−42] The usage of the comonomer DPC, rather than previously reported dialkyl carbonates, is based on the consideration that polymerization of DPC and α,ω-diols can be conducted under more practical reaction conditions and uses air-stable catalyst, exhibiting exceptional promise for scalable synthesis and further application; in contrast, dialkyl carbonates require the harsher reaction conditions due to the usage of highly active metal compounds, such as NaH and LiH,[34] which are easy to be deactivated in the presence of moisture. More importantly, DPC is typically reacted in equivalent amounts with the α,ω-diols during melt polycondensation, which is more atom-economical than dialkyl carbonate with excess addition.[23,34]

The polymerization process undergoes an transesterification process at 180 °C and a polycondensation process at 230 °C (Figure 2a). NaOH (1×10^{-4} mol %) and PPh_4OPh (2.5×10^{-3} mol %) were chosen as a catalytic system, which shows as excellent catalytic performance as the polycondensation of DPC and bisphenol A in our previous work,[43] producing high-quality polycarbonates. The presence of PPh_4OPh can enhance the reactivity in the transesterification and reduce the usage of NaOH, the residual of which reduces the thermal stability of product polycarbonates. Intriguingly, PPh_4OPh can gradually decompose and deactivate at the subsequent polycondensation phase at high temperatures (230 °C), avoiding its residual influence on the thermostability of the final products. Since the reaction process becomes mass-transfer controlled in the polycondensation stage (i.e., the removal of phenol byproduct)

https://doi.org/10.1021/acs.macromol.4c00933
Macromolecules 2024, 57, 7020−7030

rather than reaction-rate controlled due to the high viscosity, a small amount of NaOH is enough to catalyze the polycondensation. Notably, the usage of a small amount of NaOH catalyst is still necessary as using PPh_4OPh alone is difficult to drive the later-stage polycondensation reaction.[43]

The resultant PLPCs are characterized by ^{1}H NMR, ^{13}C NMR, and gel permeation chromatography (GPC). As an overview for all the resultant PLPCs, >99% carbonate linkages, weight-average molecular weight (M_w) around 10^5 g/mol, narrow molecular weight distribution ($Đ$, 1.69−1.80), and moderate to high crystallinity (38−64%) were observed (Table 1). Taking PC12 as the representative PLPC, Figures 2b and S1 present the related ^{1}H NMR and ^{13}C NMR spectra. The integration ratio of H_a [−OC(O)O−CH_2-CH$_2$−(CH$_2$)$_8$-CH$_2$−CH_2−], H_b [−OC(O)O−CH$_2$−CH_2−(CH$_2$)$_8$−CH_2−CH$_2$−], and H_c [−OC(O)O−CH$_2$−CH$_2$−(CH_2)$_8$−CH$_2$−CH$_2$−] at 4.11, 1.66, and 1.26 ppm in ^{1}H NMR spectrum conformed well to 4/4/16. In the corresponding ^{13}C NMR, the peaks at 155, 68, 29, and 26 ppm could be assigned to C_d [−OC(O)O−CH$_2$−CH$_2$−(CH$_2$)$_8$−CH$_2$−CH$_2$−], C_a [−OC(O)O−CH$_2$−CH$_2$−(CH$_2$)$_8$−CH$_2$−CH$_2$−], and C_b and C_c [−OC(O)O−CH$_2$−CH$_2$−(CH$_2$)$_8$−CH$_2$−CH$_2$−]. ^{1}H NMR and ^{13}C NMR spectra for other PLPCs are provided in Figures S2−S9 in the Supporting Information. To ensure that the molecular weights of the PLPCs are within the same order of magnitude, allowing for a more straightforward comparison of their properties, the polycondensation reactions were halted at a specific torque. This approach was chosen because the torque generated by the stirrer can roughly reflect the viscosity of the reaction system. The GPC data of all PLPCs are presented in Figure 2c, showing a unimodal and narrow peak for each polymer specimen. The detailed M_w and $Đ$ are provided in Table 1. The high molecular weights of PC6−PC14 varied from 92 to 121 kg/mol with narrow distributions were first achieved using DPC as the carbonyl source, and the synthesized high-quality PLPCs are beneficial for the subsequent melt spinning and hot-drawing processes.

Table 1. GPC Data, Thermal Properties, and Crystallinity of the PLPCs

polymer	M_w[a] (g/mol)	$Đ$[a]	T_m[b] (°C)	T_c[b] (°C)	ΔH_m[b] (J/g)	X_{WAXD}[c] (%)
PC6	92,000	1.80	51.7	12.1	27.7	38
PC8	101,000	1.69	17.6/60.6	31.5	5.8/30.4[d]	42
PC10	121,000	1.69	60.0	40.3	69.7	53
PC12	120,000	1.77	71.5	48.0	77.0	58
PC14	112,000	1.75	84.8	58.9	84.8	64

[a] M_w and $Đ$ are obtained from GPC measurements conducted at a flow rate of 1.00 mL/min at 35 °C using a linear polystyrene standard and THF as the eluent. [b] T_m and T_c were collected from the DSC heating and cooling curves after eliminating the thermal history of the specimens. ΔH_m was obtained by integrating the melting peak in the DSC curves. [c] X_{WAXD} was calculated from the deconvolution of WAXD data. [d] ΔH_m of the two melting peaks in the DSC curve of PC8.

PLPC Properties. With the well-defined and high-molecular-weight PLPCs in hand, we then investigated the thermal properties of these PLPCs, which would provide directions for further polymer processing and applications. Thermogravimetric analysis (TGA, Figure 3a) was first applied to assess the thermal stability. It shows all PLPCs present similar decomposition behavior. A slight increase in $T_{d5\%}$ (degradation temperatures corresponding to 5% mass loss, ranging from 323.5 to 350.0 °C) was observed, which correlates with a decreased density of carbonate units in the PLPC molecular chains. Meanwhile, differential thermogravimetry (DTG, Figure S10) analysis revealed that the peak

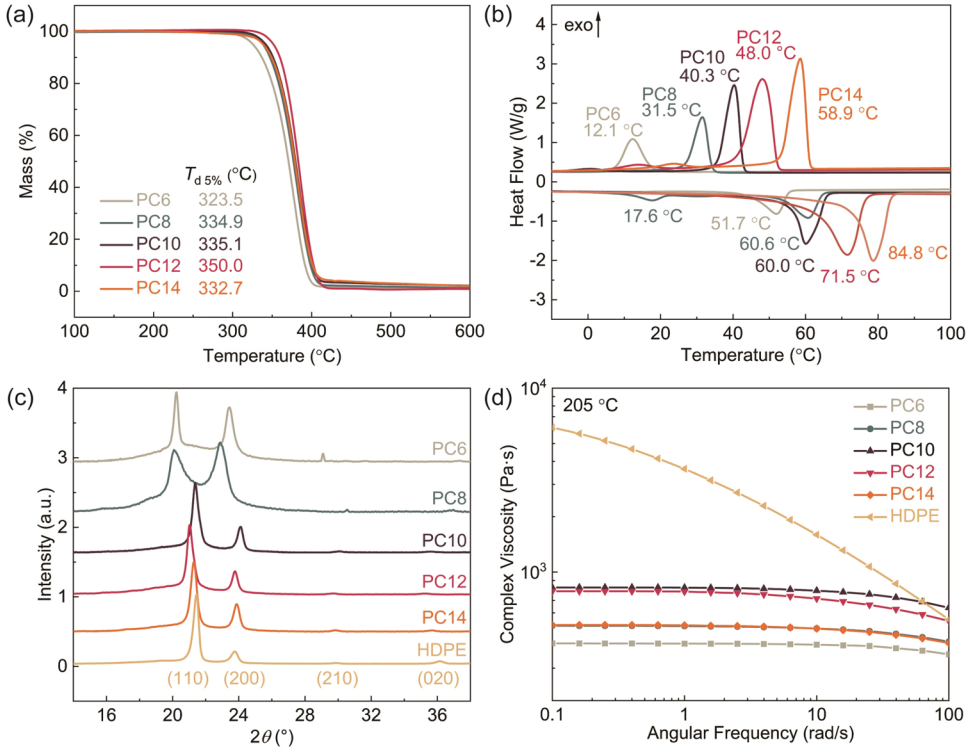

Figure 3. (a) TGA curves, (b) DSC thermograms, (c) WAXD profiles, and (d) dynamic frequency sweeps of the corresponding polymers.

https://doi.org/10.1021/acs.macromol.4c00933
Macromolecules 2024, 57, 7020−7030

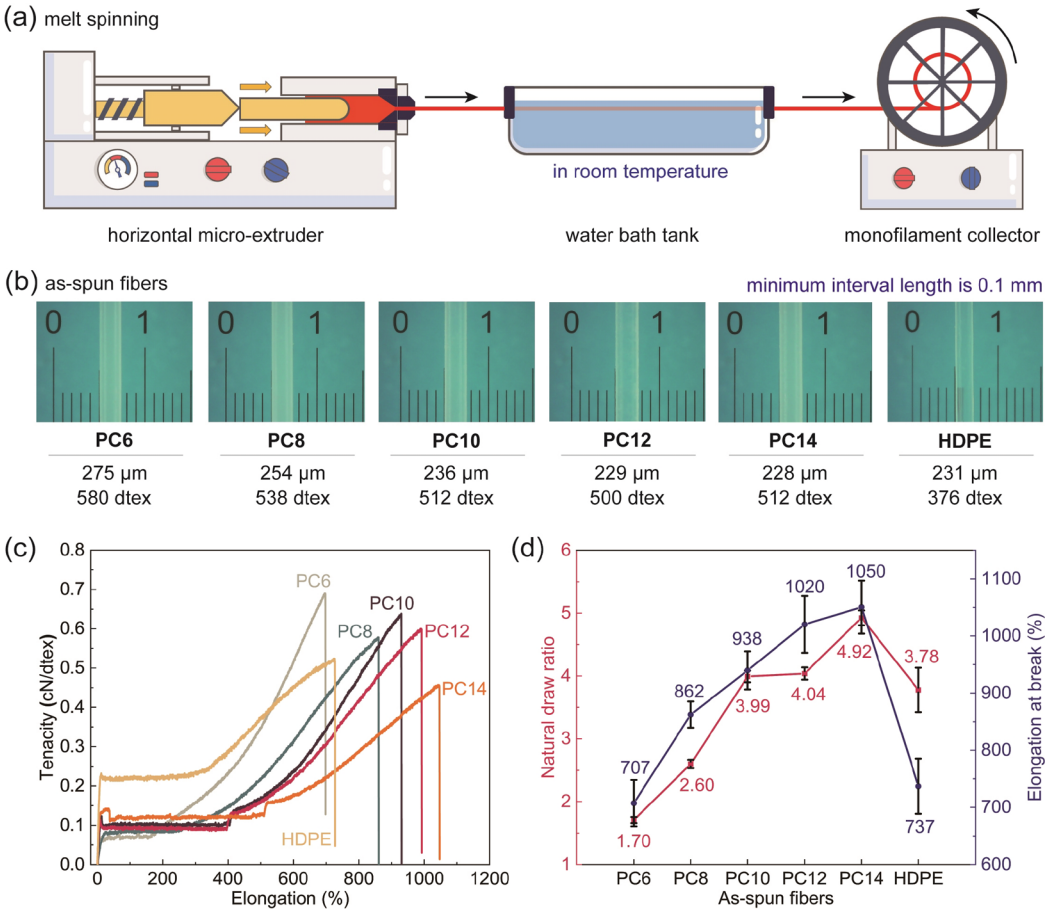

Figure 4. (a) Schematic diagram of the melt spinning process (spinning temperature: 185 °C for PC6, PC8, and PC14; 205 °C for PC10 and PC12; 280 °C for HDPE). (b) Schematic diagram of the as-spun fibers. (c) Tensile mechanical test curves. (d) Natural draw ratio and elongation at break of the as-spun fibers.

degradation rates for PLPCs (T_{peak}) were almost consistent (377.1−385.7 °C). The initial decomposition temperature is much higher than the melting temperature and molding processing temperature of PLPCs (vide infra), which can meet the requirement for processing and daily usage.

All the PLPCs were semicrystalline, and their crystal properties were initially investigated by differential scanning calorimetry (DSC) analysis (Figure 3b). The DSC curves show that both the melting temperatures (51.7−84.8 °C) and crystallization temperatures (12.1−58.9 °C) gradually increase as the density of carbonate units decreases (Figures S11 and S12). Notably, two T_m values of 17.6 and 60.6 °C can be found in PC8. This phenomenon can be ascribed to a reversible crystal−crystal transition that is similar to nylon's Brill transition, which has been systematically studied by Liu et al.[44] They have also found that only PC8 presents this unique "Brill transition" among PC3−PC10, which may be due to the delicate balance between the methylene segment mobility and the weak dipole−dipole interaction. The overall change in melting temperatures of PC6−PC14 arises from the insertion of carbonate units into the PE lattice,[45] and it can be elucidated using the inclusion model proposed by Sanchez and Eby,[46] wherein PLPCs are regarded as copolymers containing carbonate units and methylene units. This model accounts for the energy penalty associated with the presence of lattice inclusions:

$$T_m = T^0_{m,PE}\left(1 - \frac{\varepsilon}{\Delta H^0_{m,PE}}X_{CU} - \frac{2\sigma}{\Delta H^0_{m,PE} l}\right)$$

wherein T_m represents the melting temperature of the copolymers, $T^0_{m,PE}$ represents the equilibrium melting temperature of PE, X_{CU} represents the mole fraction of carbonate units [−OC(O)O−] in the copolymers, ε represents the energy penalty resulting from the reduction in crystal packing energy caused by the incorporation of carbonate units into the crystal lattice,[47] $\Delta H^0_{m,PE}$ represents the complete melting enthalpy of linear PE, σ represents the surface free energy of the crystal surface, and l represents the lamellar thickness. According to the previous research on PE-like materials, the presence of disturbing units has a negligible influence on the lamellar thickness l and surface free energy σ.[48] Therefore, the cumulative energy penalty ($\varepsilon \cdot X_{CU}$) is the main reason for the decrease in the melting temperatures for PLPCs. An increase in melting enthalpies (ΔH_m) (27.7 J/g for PC6, 5.8/30.4 J/g for PC8, 69.7 J/g for PC10, 77.0 J/g for PC12, and 84.8 J/g for PC14) with the declined carbonate unit density can be observed (Table 1). This increase in ΔH_m can be attributed to the decrease in the lattice defects caused by the incorporation of carbonate units into the crystal lattice. In addition, it can be noted in isothermal crystallization that the incorporation of carbonate units slows the crystallization rate of PLPCs (Figure S13).

https://doi.org/10.1021/acs.macromol.4c00933
Macromolecules 2024, 57, 7020−7030

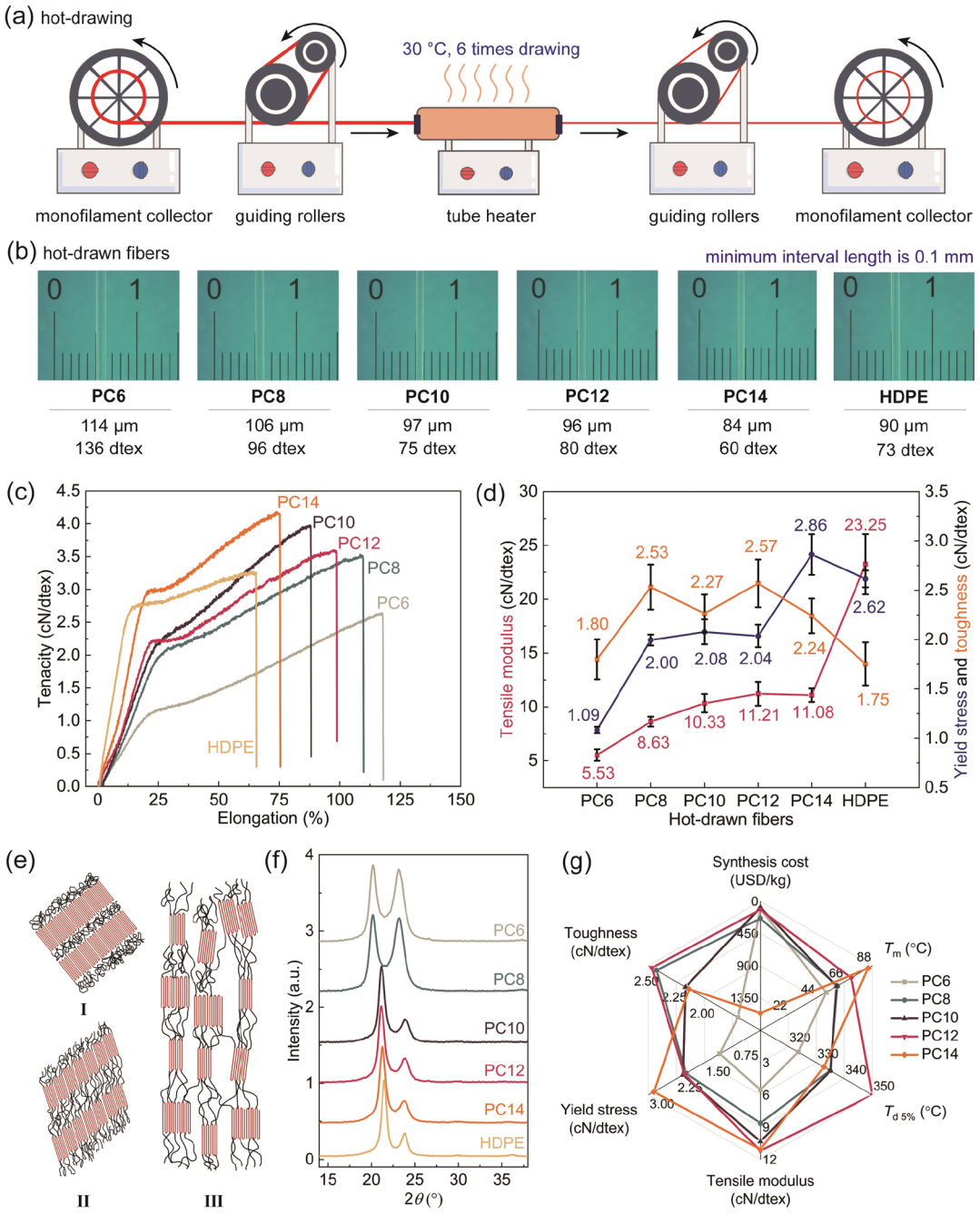

Figure 5. (a) Hot-drawing process, (b) schematic diagram, (c) tensile mechanical test curves, and (d) tensile modulus, yield stress, and toughness of the hot-drawn fibers. (e) Changes in crystal morphology of the as-spun fibers during hot-drawing. (f) WAXD curves of the hot-drawn fibers. (g) Comprehensive comparison of the synthesis cost, thermal properties, and mechanical properties between the hot-drawn PLPC fibers.

The crystalline nature of the PLPCs was further confirmed by wide-angle X-ray diffraction (WAXD) (Figure 3c). By deconvoluting the WAXD data, the crystallinity (X_{WAXD}) of PLPCs was obtained, wherein PC14 with the longest methylene segments exhibits the highest X_{WAXD} (64%) among PC6 (38%), PC8 (42%), PC10 (53%), and PC12 (58%) (Table 1). Long-methylene-segment-length PLPCs (PC10−PC14) with high crystallinity display primary reflections at 2θ angles around 21 and 24° that correspond to the (110) and (200) crystal planes of the orthorhombic crystal structure, which is analogous to high-density polyethylene (HDPE). This result indicates that these PLPCs share a folded chain platelet arrangement similar to that of HDPE in the long-range ordered crystalline region along the molecular backbone. However, an obvious shift of the 2θ angle peak positions of PC6 and PC8 was observed, which suggests the expansion along the *a* and/or *b* axes of the lattice and deviation of the unit cell from the orthorhombic crystal lattice of HDPE. Previous work of Müller and Liu has also revealed this derivation of unit cells of PC6 and PC8 with odd carbon numbers in unit structure, showing a monoclinic crystalline structure.[39] Interestingly, they also found a clear even−odd effect in terms of thermal properties and crystalline structure for PLPC with fewer methylene groups ranging from 6 to 9 and a saturation of the even−odd effect with more methylene groups ranging from 10 to 12. The excessive number of

https://doi.org/10.1021/acs.macromol.4c00933
Macromolecules 2024, 57, 7020−7030

Table 2. Crystallinity, Grain Size, and Orientation of Hot-Drawn PLPC Fibers

	$X_{WAXD,HDF}$[a]	grain size[b] (Å)				orientation	
polymer	(%)	$(110)_{virgin}$	$(200)_{virgin}$	$(110)_{HDF}$	$(200)_{HDF}$	f_C[c]	Δn[d]
PC6	56	286	155	103	68	0.925	0.0719
PC8	59	98	100	100	68	0.929	0.0694
PC10	64	192	226	110	74	0.929	0.0673
PC12	64	197	231	106	77	0.931	0.0645
PC14	62	199	201	109	73	0.942	0.0675
HDPE	73	230	176	125	98	0.940	0.0459

[a]Crystallinity ($X_{WAXD,HDF}$) was calculated from the deconvolution of WAXD curves of the hot-drawn fibers (HDF). [b]Grain sizes corresponding to the (110) and (200) crystal planes were calculated by Scherrer equation: $D = K\lambda/B \cos\theta$, D, the grain size; K, the Scherrer constant ($K = 0.89$); λ, the X-ray wavelength ($\lambda = 0.1541$ nm); B, the full width at half-maximum (fwhm) in radians of crystal plane diffraction peak; θ, the Bragg diffraction angle. [c]The (110) crystal plane orientation degree (f_C) of hot-drawn PLPC fibers was calculated from the azimuthal scan curves (Figure S33) using the empirical formula: $f_C = (360 - \Sigma H_i)/360$, H_i represents the fwhm in degrees of the peak i. [d]The Δn of hot-drawn fibers was quantified by a birefringence meter: $\Delta n = R/D$, R, the optical path difference (nm); D, the fiber diameter (nm).

carbonate units in the crystal lattice is also likely to affect the relative growth rates of the (110) and (200) crystal planes, resulting in different intensity ratios for the (110) and (200) crystal planes of PC6 and PC8 from the other samples in Figure 3c. These differentiations of the crystalline properties may influence the mechanical performance of the PLPC materials.

Next, rheological studies were conducted to assess the melt flow characteristics of the PLPCs. Initially, we conducted dynamic time sweeps at a constant frequency of 1 rad/s in a 15 min testing window to ensure the thermostability of these PLPCs (Figure S14). The dynamic frequency sweeps were then explored in a frequency range from 100 to 0.1 rad/s at 205 °C in a safe processing time window (Figure 3d). For HDPE, higher melt viscosity and strong shear thinning behavior at low frequencies can be observed due to the high molecular weight and dense packing of hydrocarbon chains causing a long relaxation time in the melt state. As for PLPCs, due to the presence of carbonate bonds, lower melt viscosity and an obvious Newtonian plateau region can be observed, and the viscosity shows low sensitivity to shear frequency. These results suggest that the molding process for PLPCs can be easily regulated by processing temperature. The above characteristic allows PLPCs to be processed at a lower temperature and lower shear frequency than HDPE, which also means less energy and power input.

Melt Spinning and Mechanical Properties of As-Spun Fibers. Synthetic polymer fibers have infiltrated modern society due to their easy structure control, low density, and high degree of flexibility. The high molecular weight, long linear molecular chain length, and crystalline structure of PLPCs suggest that they have sufficient stability and mechanical strength to meet the requirements of polymer fibers. Owing to the excellent thermal processing window (above the T_m and below T_d), as-spun PLPC fibers were obtained through melt spinning using a horizontal micro-extrusion system (Figure 4a). Wherein, the polymers were loaded into the microextruder and heated to ensure complete melting. To eliminate the impact of processing technologies on the comparison of fiber properties, a specific spinning temperature was applied for different polymers to ensure a similar melt viscosity. These optimized spinning temperatures were obtained by dynamic frequency sweep at different temperatures (Figure S15). A spinning draw ratio was set to nearly 15 times with a melt extrusion rate of 1.125 m/min at the spinneret die and a collection rate of 16.4 m/min at the disc monofilament collector. A water bath was established between the extrusion and collection unit to rapidly cool the molten fiber, preventing adhesion during the collection of the as-spun fibers. After this melting spinning process, polymer fibers with similar diameters (228−275 μm) were prepared (Figure 4b).

All as-spun fibers exhibit excellent stretchability in tensile mechanical tests (Figures 4c,d and S16−S21). The elongations at break are 707% for PC6, 862% for PC8, 938% for PC10, 1020% for PC12, 1050% for PC14, and 737% for HDPE. These fibers all show a cold drawing phenomenon like yielding and form necking due to the high crystallinity during the drawing process, even though the T_gs of these fibers are below room temperature. The natural draw ratio at which the fiber undergoes plastic deformation until complete necking was determined: 1.70 (PC6), 2.60 (PC8), 3.99 (PC10), 4.04 (PC12), 4.92 (PC14), 3.78 (HDPE). Unfolding and orientation of the crystal folding chains account for the occurrence of the plastic deformation, since the as-spun PLPC fibers with more crystal folding chains (i.e., higher crystallinity) typically exhibit a larger natural draw ratio and elongation at break. However, HDPE with the highest crystallinity shows a downward trend in natural draw ratio and elongation at break compared to PLPCs. This can be attributed to the carbonate units in PLPCs acting as flexible units and enhancing the slip between molecular chains during drawing.

Overall, the axial mechanical strengths of these as-spun PLPC fibers (Figure 4c) are unsatisfying due to the entropic elasticity of molecular chains during melt spinning. Even if a high spinning draw ratio (15:1) was applied, the molecular chains cannot form an effective fiber axial orientation structure, although it can affect the thickness of the as-spun fibers. This is due to the entropic elasticity of the polymer in the molten state, where the polymer melt extruded from the spinneret tends to release the internal stresses in the melt to counteract the orientation.[49] When these unoriented as-spun PLPC fibers are subjected to external force along the axial direction, the smaller intermolecular forces between the molecular chains are difficult to resist, making the fiber prone to deformation. To overcome these issues, a further hot-drawing process is required to improve the mechanical properties of the PLPC fibers.

Structure and Properties of Hot-Drawn Fibers. The as-spun fibers were then drawn at 30 °C in a hot-drawing apparatus to force the molecular chains to orient along the axis and thereby enhance the axial strength of the fibers (Figure

https://doi.org/10.1021/acs.macromol.4c00933
Macromolecules 2024, 57, 7020−7030

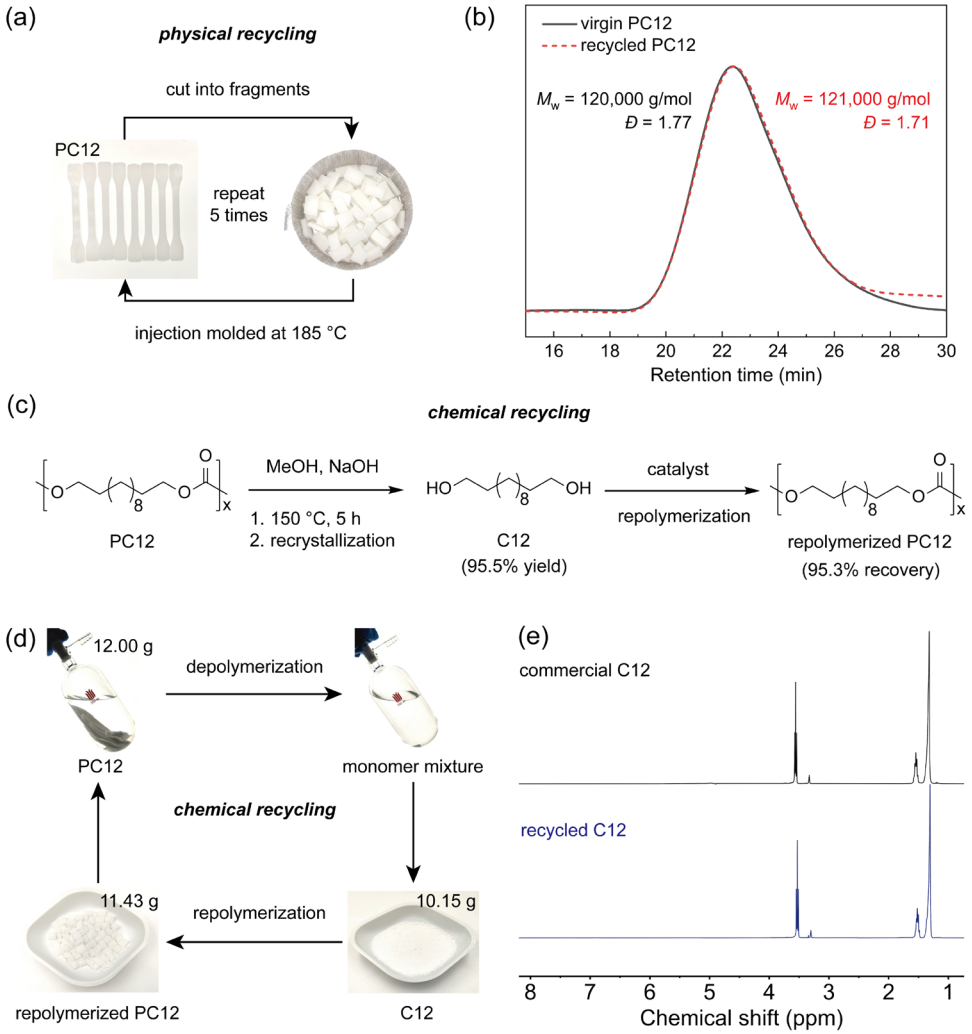

Figure 6. (a) Physical recycling process of PC12. (b) GPC traces of virgin PC12 and recycled PC12 after the fifth processing cycle. (c) Schematic overview of the chemical recycling of PC12 via alcoholysis and repolymerization. (d) Multigram-scale chemical recycling of PC12. (e) ^{1}H NMR spectra of commercial C12 and recycled C12.

5a). To ensure the full development of plastic deformation of all as-spun fibers during the hot-drawing process, the drawing ratio was set to 6:1, which is higher than the natural draw ratio of all as-spun fibers. After the hot-drawing process, the cross-sectional area is about 6 times smaller than that of as-spun fibers with fiber diameters of 84−114 μm. Additionally, the linear densities of these hot-drawn fibers are also given in Figure 5b. It should be mentioned that the molecular weight of all PLPCs did not change significantly after being thermally processed into hot-drawn fibers (Figures S22 and S26), which ensures stability and reliability of mechanical testing of hot-drawn fibers.

Tensile mechanical tests of the hot-drawn fibers were then performed. In contrast to the as-spun fibers, the hot-drawn fibers exhibit about 3−10-fold enhanced tensile strength (Figure 5c,d) due to the deformation of crystals (Figure 5e), the formation of smaller grain sizes, the increased crystallinity (Figure 5f), and the generation of overall molecular chain orientation (Table 2). The toughness of these hot-drawn PLPC fibers (1.80−2.57 cN/dtex) was largely promoted by introducing carbonate units into the HDPE (1.75 cN/dtex) backbones (Figure 5d), which benefits the durability of PLPC fibers. It can also be observed that the tensile modulus increases obviously from PC6 to PC10 with a decrease in the carbonate unit density (PC6:5.53 cN/dtex, PC8:8.63 cN/dtex, PC10:10.33 cN/dtex). Also, it becomes leveled off from PC10 to PC12 (11.21 cN/dtex) and PC14 (11.08 cN/dtex). Even though the tensile modulus of all these hot-drawn PLPC fibers is lower than that of HDPE (23.25 cN/dtex), they still meet the requirement in daily life usage. Additionally, the yield stress of these hot-drawn PLPC fibers of (PC8−PC14) is comparable to that of HDPE. Especially, yield stress of PC14 (2.86 cN/dtex) is even higher than that of HDPE (2.62 cN/dtex), indicating its good performance against destruction. The compromised tensile modulus and yield stress of the short-methylene-sequence hot-drawn PLPC fibers may be due to the excessive carbonate defective units causing lattice distortion and moderate crystallinity, as measured in WAXD.

We also measured the orientation degree (f_C) of the crystal region of the hot-drawn fibers by azimuthal scanning and the overall orientation degree of the molecular chain segments by birefringence (Δn) (Figure S33, Table 2). Comparing to other PLPCs (f_C ranging from 0.929 to 0.940, and Δn ranging from 0.0459 to 0.0673), PC6 and PC8 show similar orientation degree of the crystal region (f_C = 0.925 and 0.929, respectively) but obvious higher overall orientation degree

https://doi.org/10.1021/acs.macromol.4c00933
Macromolecules 2024, 57, 7020−7030

(Δn = 0.0719 and 0.0694, respectively). While the overall orientation degree is the overall reflection of the orientation of amorphous region and crystal region,[50] these results suggest the high orientation degree of amorphous region of PC6 and PC8 at the same hot-drawn ratio. The molecular chains in the higher orientation amorphous region of PC6 and PC8 are more likely to dissipate energy by sliding under external forces, resulting in a compromised stress resistance.

A comprehensive comparison of hot-drawn PLPC fibers in aspects of synthesis cost, thermal properties, and mechanical properties is visually presented in a radar chart (Figure 5g). Among them, PC12, which has an outstanding integration of yield stress, tensile modulus, toughness, synthetic cost, heat resistance ($T_{d5\%}$), and processability (process window, $T_{d5\%}$, $\sim T_m$), holds attractive potential applications. In summary, all these mechanical and thermal performances as well as the synthesis cost suggest that the hot-drawn PLPC fibers are promising materials with better suitability than HDPE in some cases, due to their improved toughness, degradability, and the easily tunable mechanical properties by changing the carbonate unit density.

Physical Recycling and Chemical Recycling of PLPCs. Polymers that can be reprocessed with retention of properties have advantages in facilitating end-of-life treatment, as energy inputs can be significantly reduced.[51] The reprocessing ability of PLPCs was investigated by using PC12 as a model polymer. PC12 was cut into fragments and injection-molded at 185 °C to form tensile test specimens. The tensile specimens were subjected to five processing cycles of repeated cutting and injection molding (Figure 6a), and the mechanical properties of the specimens obtained from the first and fifth injection moldings were tested. After the fifth processing cycle, the appearance of the polymer was unchanged and remained white semicrystalline (Figure S35). More importantly, the molecular weight of the final recycled PC12 specimen has not changed compared to the virgin polymer (Figure 6b). Similar results can also obtained by repeatedly chopping and hot-pressing at higher temperatures seven times (Figure S34). Simultaneously, the mechanical properties of the tensile specimens obtained from the first and fifth injection moldings show no significant changes (Figure S35). These results demonstrate the enormous potential of efficient recycling of both PLPC manufacturing scraps and even waste samples by physical recycling protocols without any undesirable material decomposition.

Furthermore, we examined the chemical recyclability of the polymers, which present a powerful tool for circularizing the plastic economy, as it can not only reduce the need for continuous feedstock sourcing but also eliminate the accumulation of plastic waste.[52] With the in-chain carbonate units, the chemical recycling of PLPC monomers can be easily enabled by alcoholysis. A multigram-scale alcoholysis of PC12 was conducted using NaOH as a catalyst and methanol as a reactant at 150 °C for 5 h (Figures 6c,d and S36). After concentration and recrystallization, the C12 monomer was isolated in a 95.5% yield and showed a high purity, as demonstrated by ^{1}H NMR spectroscopy (Figure 6e). Meanwhile, the other product dimethyl carbonates can also be recycled to produce DPC, which is a well-established process in the industry.[23] The recovered monomer C12 could be directly repolymerized with DPC to produce well-defined PC12 without compromising the reactivity. The repolymerized PC12 shows comparable or slightly higher molecular weight than that of the virgin PC12 (Figure S37). These results supported the establishment of the monomer−polymer−monomer life cycle of PLPCs. Chemical recycling of other PLPCs was also performed to generate the corresponding α,ω-diols (Figures S38−S41). Wherein, it can be observed that carbonate units promote alcoholysis since an increasing reaction time was needed for PLPCs with longer methylene sequences (Figure S42, Table S1). The chemical recyclability of the PLPCs can validate their recycling from future composite materials.

CONCLUSIONS

In summary, a series of PLPCs (PC6−PC14) were synthesized using equivalent biobased aliphatic diols and diphenyl carbonate via melt polycondensation. These PLPCs present high molecular weights (92,000−121,000 g/mol) and narrow distributions (1.69−1.80) with high yield (~99%). The effects of the carbonate unit density on thermal, crystal, and mechanical properties were systematically studied. Furthermore, fibers of these PLPCs were first prepared by undergoing melt spinning and the hot-drawing process under optimized conditions. The long-spaced PLPC (PC10, PC12, and PC14) fibers exhibit an admirable tensile modulus, yield stress, and toughness. It can be concluded that the $-OCOO-(CH_2)_{10}-$ carbonate unit (PC10) is the shortest methylene sequence length to maintain the PE-like properties, while PC12 outperformed the other PLPCs in terms of overall performance. These PLPCs also show excellent physical and chemical recyclability. These results indicate that PLPC fiber is a promising alternative to HDPE fiber, especially suitable for applications involving fiber materials with short life cycles, such as nonwoven fabrics used in disposable medical products and disposable fiber packaging materials. In the future, sustainable PE-like polymers are expected to show excellent and tunable performance to replace current petrochemical plastics and fibers.

ASSOCIATED CONTENT

Supporting Information

The Supporting Information is available free of charge at https://pubs.acs.org/doi/10.1021/acs.macromol.4c00933.

Experimental procedures, additional figures and tables, NMR spectra, GPC traces, DTG, DSC, rheological tests, tensile mechanical tests, WAXD, and additional experimental details (PDF)

AUTHOR INFORMATION

Corresponding Authors

Yao-Yao Zhang − *National Engineering Laboratory for Textile Fiber Materials and Processing Technology (Zhejiang), School of Materials Science and Engineering, Zhejiang Sci-Tech University, Hangzhou 310018, China;* orcid.org/0000-0002-8031-9139; Email: zhangyy@zstu.edu.cn

Xianming Zhang − *National Engineering Laboratory for Textile Fiber Materials and Processing Technology (Zhejiang), School of Materials Science and Engineering, Zhejiang Sci-Tech University, Hangzhou 310018, China; Zhejiang Provincial Innovation Centre of Advanced Textile Technology, Shaoxing 312000, China;* orcid.org/0000-0002-4653-2630; Email: zhangxm@zstu.edu.cn

https://doi.org/10.1021/acs.macromol.4c00933
Macromolecules 2024, 57, 7020−7030

Authors

Mingfu Zheng − *National Engineering Laboratory for Textile Fiber Materials and Processing Technology (Zhejiang), School of Materials Science and Engineering, Zhejiang Sci-Tech University, Hangzhou 310018, China*

Wenjun Peng − *National Engineering Laboratory for Textile Fiber Materials and Processing Technology (Zhejiang), School of Materials Science and Engineering, Zhejiang Sci-Tech University, Hangzhou 310018, China; Zhejiang Provincial Innovation Centre of Advanced Textile Technology, Shaoxing 312000, China;* orcid.org/0009-0001-3235-3279

Wenxing Chen − *National Engineering Laboratory for Textile Fiber Materials and Processing Technology (Zhejiang), School of Materials Science and Engineering, Zhejiang Sci-Tech University, Hangzhou 310018, China;* orcid.org/0000-0002-4554-1455

Complete contact information is available at: https://pubs.acs.org/10.1021/acs.macromol.4c00933

Notes

The authors declare no competing financial interest.

■ ACKNOWLEDGMENTS

This work was supported by National Natural Science Foundation of China (Grants 51973196 and 22301279).

■ REFERENCES

(1) U. N. Environment Programme *Drowning in Plastics − Marine Litter and Plastic Waste Vital Graphics*. UNEP - UN Environment Programme http://www.unep.org/resources/report/drowning-plastics-marine-litter-and-plastic-waste-vital-graphics 2021.

(2) Geyer, R.; Jambeck, J. R.; Law, K. L. Production, Use, and Fate of All Plastics Ever Made. *Sci. Adv.* **2017**, *3* (7), No. e1700782.

(3) Westlie, A. H.; Chen, E. Y.-X.; Holland, C. M.; Stahl, S. S.; Doyle, M.; Trenor, S. R.; Knauer, K. M. Polyolefin Innovations toward Circularity and Sustainable Alternatives. *Macromol. Rapid Commun.* **2022**, *43* (24), 2200492.

(4) Schaller, R.; Feldman, K.; Smith, P.; Tervoort, T. A. High-Performance Polyethylene Fibers "Al Dente": Improved Gel-Spinning of Ultrahigh Molecular Weight Polyethylene Using Vegetable Oils. *Macromolecules* **2015**, *48* (24), 8877−8884.

(5) Lu, J.; Sue, H.-J. Characterization of Crystalline Texture of LLDPE Blown Films Using X-Ray Pole Figures. *Macromolecules* **2001**, *34* (6), 2015−2017.

(6) Ragaert, K.; Delva, L.; Van Geem, K. Mechanical and Chemical Recycling of Solid Plastic Waste. *Waste Manag.* **2017**, *69*, 24−58.

(7) Eagan, J. M.; Xu, J.; Di Girolamo, R.; Thurber, C. M.; Macosko, C. W.; LaPointe, A. M.; Bates, F. S.; Coates, G. W. Combining Polyethylene and Polypropylene: Enhanced Performance with PE/*i*PP Multiblock Polymers. *Science* **2017**, *355* (6327), 814−816.

(8) Jambeck, J. R.; Geyer, R.; Wilcox, C.; Siegler, T. R.; Perryman, M.; Andrady, A.; Narayan, R.; Law, K. L. Plastic Waste Inputs from Land into the Ocean. *Science* **2015**, *347* (6223), 768−771.

(9) Bergmann, M.; Collard, F.; Fabres, J.; Gabrielsen, G. W.; Provencher, J. F.; Rochman, C. M.; van Sebille, E.; Tekman, M. B. Plastic Pollution in the Arctic. *Nat. Rev. Earth Environ.* **2022**, *3* (5), 323−337.

(10) Arroyave, A.; Cui, S.; Lopez, J. C.; Kocen, A. L.; LaPointe, A. M.; Delferro, M.; Coates, G. W. Catalytic Chemical Recycling of Post-Consumer Polyethylene. *J. Am. Chem. Soc.* **2022**, *144* (51), 23280−23285.

(11) Sun, J.; Bubel, K.; Chen, F.; Kissel, T.; Agarwal, S.; Greiner, A. Nanofibers by Green Electrospinning of Aqueous Suspensions of Biodegradable Block Copolyesters for Applications in Medicine, Pharmacy and Agriculture. *Macromol. Rapid Commun.* **2010**, *31* (23), 2077−2083.

(12) Li, X.; Clarke, R. W.; An, H.; Gowda, R. R.; Jiang, J.; Xu, T.; Chen, E. Y. -X. Dual Recycling of Depolymerization Catalyst and Biodegradable Polyester That Markedly Outperforms Polyolefins. *Angew. Chem., Int. Ed.* **2023**, *62* (26), No. e202303791.

(13) Abel, B. A.; Snyder, R. L.; Coates, G. W. Chemically Recyclable Thermoplastics from Reversible-Deactivation Polymerization of Cyclic Acetals. *Science* **2021**, *373* (6556), 783−789.

(14) Stempfle, F.; Ortmann, P.; Mecking, S. Long-Chain Aliphatic Polymers To Bridge the Gap between Semicrystalline Polyolefins and Traditional Polycondensates. *Chem. Rev.* **2016**, *116* (7), 4597−4641.

(15) Janani, H.; Marxsen, S. F.; Eck, M.; Mecking, S.; Tashiro, K.; Alamo, R. G. Polymorphism and Stretch-Induced Transformations of Sustainable Polyethylene-like Materials. *ACS Macro Lett.* **2024**, *13* (2), 201−206.

(16) Myers, D.; Witt, T.; Cyriac, A.; Bown, M.; Mecking, S.; Williams, C. K. Ring Opening Polymerization of Macrolactones: High Conversions and Activities Using an Yttrium Catalyst. *Polym. Chem.* **2017**, *8* (37), 5780−5785.

(17) Van Der Meulen, I.; De Geus, M.; Antheunis, H.; Deumens, R.; Joosten, E. A. J.; Koning, C. E.; Heise, A. Polymers from Functional Macrolactones as Potential Biomaterials: Enzymatic Ring Opening Polymerization, Biodegradation, and Biocompatibility. *Biomacromolecules* **2008**, *9* (12), 3404−3410.

(18) De Geus, M.; Van Der Meulen, I.; Goderis, B.; Van Hecke, K.; Dorschu, M.; Van Der Werff, H.; Koning, C. E.; Heise, A. Performance Polymers from Renewable Monomers: High Molecular Weight Poly(Pentadecalactone) for Fiber Applications. *Polym. Chem.* **2010**, *1* (4), 525−533.

(19) Ortmann, P.; Heckler, I.; Mecking, S. Physical Properties and Hydrolytic Degradability of Polyethylene-like Polyacetals and Polycarbonates. *Green Chem.* **2014**, *16* (4), 1816.

(20) Ortmann, P.; Mecking, S. Long-Spaced Aliphatic Polyesters. *Macromolecules* **2013**, *46* (18), 7213−7218.

(21) Eck, M.; Schwab, S. T.; Nelson, T. F.; Wurst, K.; Iberl, S.; Schleheck, D.; Link, C.; Battagliarin, G.; Mecking, S. Biodegradable High-Density Polyethylene-like Material. *Angew. Chem., Int. Ed.* **2023**, *62* (6), No. e202213438.

(22) Sun, J.; Kuckling, D. Synthesis of High-Molecular-Weight Aliphatic Polycarbonates by Organo-Catalysis. *Polym. Chem.* **2016**, *7* (8), 1642−1649.

(23) Fukuoka, S.; Fukawa, I.; Adachi, T.; Fujita, H.; Sugiyama, N.; Sawa, T. Industrialization and Expansion of Green Sustainable Chemical Process: A Review of Non-Phosgene Polycarbonate from CO_2. *Org. Process Res. Dev.* **2019**, *23* (2), 145−169.

(24) Chikkali, S.; Mecking, S. Refining of Plant Oils to Chemicals by Olefin Metathesis. *Angew. Chem., Int. Ed.* **2012**, *51* (24), 5802−5808.

(25) Mecking, S. Polyethylene-like Materials from Plant Oils. *Philos. Trans. R. Soc. Math. Phys. Eng. Sci.* **2020**, *378* (2176), 20190266.

(26) Biermann, U.; Bornscheuer, U.; Meier, M. A. R.; Metzger, J. O.; Schäfer, H. J. Oils and Fats as Renewable Raw Materials in Chemistry. *Angew. Chem., Int. Ed.* **2011**, *50* (17), 3854−3871.

(27) Zimmerer, J.; Williams, L.; Pingen, D.; Mecking, S. Mid-Chain Carboxylic Acids by Catalytic Refining of Microalgae Oil. *Green Chem.* **2017**, *19* (20), 4865−4870.

(28) Jang, Y.-J.; Nguyen, S.; Hillmyer, M. A. Chemically Recyclable Linear and Branched Polyethylenes Synthesized from Stoichiometrically Self-Balanced Telechelic Polyethylenes. *J. Am. Chem. Soc.* **2024**, *146* (7), 4771−4782.

(29) Xia, Y.; Yue, X.; Sun, Y.; Zhang, C.; Zhang, X. Chemically Recyclable Polyethylene-like Sulfur-Containing Plastics from Sustainable Feedstocks. *Angew. Chem., Int. Ed.* **2023**, *62* (13), No. e202219251.

(30) Parke, S. M.; Lopez, J. C.; Cui, S.; LaPointe, A. M.; Coates, G. W. Polyethylene Incorporating Diels−Alder Comonomers: A "Trojan Horse" Strategy for Chemically Recyclable Polyolefins. *Angew. Chem., Int. Ed.* **2023**, *62* (30), No. e202301927.

(31) Zhai, L.; Li, G.; Xu, Y.; Xiao, M.; Wang, S.; Meng, Y. Poly(Propylene Carbonate)/Aluminum Flake Composite Films with Enhanced Gas Barrier Properties. *J. Appl. Polym. Sci.* **2015**, *132* (11), 41663.
(32) Yan, H.; Cannon, W. R.; Shanefield, D. J. Thermal Decomposition Behaviour of Poly(Propylene Carbonate). *Ceram. Int.* **1998**, *24* (6), 433−439.
(33) Scharfenberg, M.; Hilf, J.; Frey, H. Functional Polycarbonates from Carbon Dioxide and Tailored Epoxide Monomers: Degradable Materials and Their Application Potential. *Adv. Funct. Mater.* **2018**, *28* (10), 1704302.
(34) Häußler, M.; Eck, M.; Rothauer, D.; Mecking, S. Closed-Loop Recycling of Polyethylene-like Materials. *Nature* **2021**, *590* (7846), 423−427.
(35) Tay, B.; van Meurs, M.; Tan, J.; Ye, S.; Borgna, A.; van Herk, A. M.; Selvaratnam, S.; Wang, C.; Taniguchi, S.; Suzuki, Y.; Utsunomiya, M.; Ito, M.; Monden, T.; Shibata, H.; Tomita, S. Imidazolium-Catalyzed Formation of Bisphenol a Polycarbonate with a Reduced Level of Branching. *Ind. Eng. Chem. Res.* **2021**, *60* (49), 17928−17941.
(36) Wang, Z.; Yang, X.; Liu, S.; Hu, J.; Zhang, H.; Wang, G. One-Pot Synthesis of High-Molecular-Weight Aliphatic Polycarbonates via Melt Transesterification of Diphenyl Carbonate and Diols Using $Zn(OAc)_2$ as a Catalyst. *RSC Adv.* **2015**, *5* (106), 87311−87319.
(37) Su, W.; Feng, J.; Wang, H.; Zhang, X.; Zhuo, R. Controllable Preparation of Poly(Alkylene Carbonate)s and Observation on Their Structure-Related Odd−Even Effect. *Polymer* **2010**, *51* (5), 1010−1015.
(38) Meabe, L.; Lago, N.; Rubatat, L.; Li, C.; Müller, A. J.; Sardon, H.; Armand, M.; Mecerreyes, D. Polycondensation as a Versatile Synthetic Route to Aliphatic Polycarbonates for Solid Polymer Electrolytes. *Electrochim. Acta* **2017**, *237*, 259−266.
(39) Pérez-Camargo, R. A.; Meabe, L.; Liu, G.; Sardon, H.; Zhao, Y.; Wang, D.; Müller, A. J. Even−Odd Effect in Aliphatic Polycarbonates with Different Chain Lengths: From Poly (Hexamethylene Carbonate) to Poly (Dodecamethylene Carbonate). *Macromolecules* **2021**, *54* (1), 259−271.
(40) Ahsan, M.; Sung, S.; Jeon, H.; Patil, M.; Chung, T.; Yun, H. Biosynthesis of Medium- to Long-Chain α,ω-Diols from Free Fatty Acids Using CYP153A Monooxygenase, Carboxylic Acid Reductase, and E. Coli Endogenous Aldehyde Reductases. *Catalysts* **2018**, *8* (1), 4.
(41) Schaffer, S.; Haas, T. Biocatalytic and Fermentative Production of α,ω-Bifunctional Polymer Precursors. *Org. Process Res. Dev.* **2014**, *18* (6), 752−766.
(42) Scheps, D.; Honda Malca, S.; Hoffmann, H.; Nestl, B. M.; Hauer, B. Regioselective ω-Hydroxylation of Medium-Chain n-Alkanes and Primary Alcohols by CYP153 Enzymes from Mycobacterium Marinum and Polaromonas Sp. Strain JS666. *Org. Biomol. Chem.* **2011**, *9* (19), 6727.
(43) Zheng, M.; Chen, M.; Zhang, L.; Peng, W.; Zhang, X.; Chen, W. Effects of Alkali Metal Catalysts on the Melt Fluidity of Polycarbonates with Different Degrees of Polymerization. *J. Appl. Polym. Sci.* **2023**, *140* (10), No. e53587.
(44) Zhao, T.; Ren, X.; Zhu, W.; Liang, Y.; Li, C.; Men, Y.; Liu, C.; Chen, E. Brill Transition" Shown by Green Material Poly-(Octamethylene Carbonate). *ACS Macro Lett.* **2015**, *4* (3), 317−321.
(45) Menges, M. G.; Penelle, J.; Le Fevere De Ten Hove, C.; Jonas, A. M.; Schmidt-Rohr, K. Characterization of Long-Chain Aliphatic Polyesters: Crystalline and Supramolecular Structure of PE22,4 Elucidated by X-Ray Scattering and Nuclear Magnetic Resonance. *Macromolecules* **2007**, *40* (24), 8714−8725.
(46) Sanchez, I. C.; Eby, R. K. Thermodynamics and Crystallization of Random Copolymers. *Macromolecules* **1975**, *8* (5), 638−641.
(47) Crist, B. Thermodynamics of Statistical Copolymer Melting. *Polymer* **2003**, *44* (16), 4563−4572.
(48) Pepels, M. P. F.; Hansen, M. R.; Goossens, H.; Duchateau, R. From Polyethylene to Polyester: Influence of Ester Groups on the Physical Properties. *Macromolecules* **2013**, *46* (19), 7668−7677.
(49) Masuda, M.; Takarada, W.; Kikutani, T. Effect of the Control of Polymer Flow in the Vicinity of Spinning Nozzle on Mechanical Properties of Poly(Ethylene Terephthalate) Fibers. *Int. Polym. Process.* **2010**, *25* (2), 159−169.
(50) Chappel, F. P. Orientation of Amorphous and Crystalline Regions in Nylon 66 Filaments. *Polymer* **1960**, *1*, 409−417.
(51) Cosate de Andrade, M. F.; Souza, P. M. S.; Cavalett, O.; Morales, A. R. Life Cycle Assessment of Poly(Lactic Acid) (PLA): Comparison between Chemical Recycling, Mechanical Recycling and Composting. *J. Polym. Environ.* **2016**, *24* (4), 372−384.
(52) Rosetto, G.; Vidal, F.; McGuire, T. M.; Kerr, R. W. F.; Williams, C. K. High Molar Mass Polycarbonates as Closed-Loop Recyclable Thermoplastics. *J. Am. Chem. Soc.* **2024**, *146* (12), 8381−8393.

https://doi.org/10.1021/acs.macromol.4c00933
Macromolecules 2024, 57, 7020−7030